SUSC 12514
6 October 2001 Disk used
ARTICLE IN PRESS
No. of Pages 8, DTD = 4.2.0
SPS, Chennai

ELSEVIER
Surface Science xxx (2001) xxx–xxx
SURFACE SCIENCE
www.elsevier.com/locate/susc

Hydrogen atoms as a probe of the optical anisotropy of indium phosphide (0 0 1)

D.C. Law, Q. Fu, S.B. Visbeck, Y. Sun, C.H. Li, R.F. Hicks *

Department of Chemical Engineering, University of California (UCLA), 405 Hilgard Avenue, Los Angeles, CA 90095-1592, USA

Received 27 April 2001; accepted for publication 29 August 2001

Abstract

The reflectance difference spectra of the InP(0 0 1) (2 × 1) and $\delta(2\times 4)$ reconstructions have been characterized using hydrogen as a probe of the surface bonds. Bands observed at 1.9, 3.1, 4.1, and 4.6 eV on the (2 × 1) and at 2.8, 3.7, and 4.6 eV on the $\delta(2\times 4)$ decrease in direct proportion to the hydrogen coverage. By comparing the changes in the reflectance difference spectra to the changes in the atomic structure of the surfaces, it is possible to relate the peaks to transitions involving specific valence bond states. © 2001 Published by Elsevier Science B.V.

Keywords: Chemical vapor deposition; Hydrogen atoms; Indium phosphide; Models of surface chemical reactions; Surface electronic phenomena; Surface structure

1. Introduction

Epitaxially grown III–V compound semiconductors have found wide application in electronic and photonic devices used in broadband communication systems. The surfaces of these materials are of great importance because they mediate the chemical reactions that occur during thin film deposition and etching. Reflectance difference spectroscopy (RDS) is a promising tool for monitoring compound semiconductor surfaces during processing [1–10]. This technique measures the difference in the near-normal reflectance of light polarized along the [1 1 0] and [$\bar{1}$ 1 0] crystal axis. The optical spectra contain a series of bands arising from the orthogonal arrangement of the group III and V surface bonds. Much work has been dedicated to clarifying the origin of the reflectance anisotropy. However, a debate has arisen over the assignments of the bands, since it is difficult to link these features to specific transitions among the valence states [7,11,12]. Recently, first-principles total energy calculations have been employed to identify the origin of the spectral features [13,14]. In addition, benchmarking RD spectra against scanning tunneling micrographs of the surfaces has helped to resolve some of these issues [7,15–18].

In the last four years, reflectance difference spectra have been reported for indium phosphide (0 0 1) reconstructions [1–5]. The two surface structures of main interest are the phosphorus-rich (2 × 1) and the indium-rich $\delta(2\times 4)$ [18,19]. In the case of the $\delta(2\times 4)$, first-principles calculations have suggested that the strong negative anisotropy

---

* Corresponding author. Tel.: +1-310-206-6865; fax: +1-310-206-4107.
E-mail address: rhicks@ucla.edu (R.F. Hicks).

PII: S0039-6028(01)01601-6

observed at 1.8 eV is due to an electronic transition between the indium–indium back bonds and the empty dangling orbitals localized at the surface indium atoms [20]. On the other hand, the origin of the features appearing in the spectra above 3.0 eV remain unresolved. With regard to the (2×1) RD spectrum, no calculations have been performed, and only tentative assignments have been made for a few peaks. Since the (2×1) is most likely present during vapor-phase epitaxy [21], it is important to understand the reflectance difference spectrum for this surface. Moreover, considerable variations in the line shapes of the optical spectra are seen when one study is compared to another, and these discrepancies need to be resolved.

In this paper, we present a useful approach to investigating the optical anisotropy of compound semiconductor surfaces. Hydrogen atoms are adsorbed onto the crystal while recording the RDS data. The H atoms attach to the dangling bonds and cleave the dimer bonds, thereby causing dramatic changes in the reflectance difference signals. This process occurs without altering the phosphorus or indium coverage on the surface [22,23]. We have used this approach to examine the optical response of the (2×1) and $\delta(2 \times 4)$ reconstructions of indium phosphide (0 0 1). It has been found that many of the bands can be linked to specific valence bond states on the surface, and that the band intensities decrease in direct proportional to the hydrogen coverage.

2. Experimental methods

Indium phosphide films, approximately 0.20 μm thick, were grown on nominally flat n-type InP(0 0 1) substrates in a horizontal metalorganic vapor-phase epitaxy reactor. The temperature during growth was 535 °C and the total reactor pressure was 20 Torr. Trimethylindium (TMIn) and tertiarybutylphosphine (TBP) were used to deposit the films with a partial pressure of 6.5×10^{-4} and 13×10^{-2} Torr, respectively. After deposition, the TBP and hydrogen flows were maintained until the samples were cooled to 300 and 40 °C, respectively. Then the InP crystals were transferred directly to an ultrahigh vacuum system for surface analysis [24]. Inside the UHV system, the InP crystals were heated to 300 and 500 °C for 30 min to create the (2×1) and $\delta(2 \times 4)$ reconstructions, respectively. Once the samples had cooled to 25 °C, the ordering of the InP surfaces were characterized by a Princeton Instruments low-energy electron diffractometer (LEED). In addition, the (2×1) and $\delta(2 \times 4)$ reconstructions were monitored with an instruments SA J-Y Nisel reflectance difference spectrometer during exposure to hydrogen [17,18]. The reflectance difference signal, $\mathrm{Re}(\Delta R/R)$, corresponds to the real part of $[(R_{[\bar{1}\,1\,0]} - R_{[1\,1\,0]})/\langle R \rangle]$. Baseline drift was subtracted from the spectrum by taking the average of two RDS spectra collected with the polarizing axis oriented +45° and −45° relative to the $[\bar{1}\,1\,0]$. Periodically during hydrogen dosing, the surface structure was checked by low-energy electron diffraction. Note that the atomic hydrogen did not etch away the phosphorus in the experimental conditions employed. The surface composition determined by X-ray photoelectron spectroscopy after hydrogen dosing is identical to that measured beforehand.

3. Results

Presented in Fig. 1(a) are a series of reflectance difference spectra obtained during hydrogen atom dosing of the (2×1) reconstruction. The arrows point to the direction of change with increasing dosage, and also indicate what happens to the LEED pattern. The half-order spots in the (2×1) LEED pattern disappear at about 100 L of H_2 (1.0 L $= 10^{-6}$ Torr s), and are converted into a (1×1) pattern at 500 L of H_2. The RDS spectra of the clean surface contain a sharp negative peak at 1.9 eV, an intense positive peak at 3.1 eV, and two positive overlapping bands at 4.1 and 4.6 eV. These latter bands appear to be superimposed on a negative feature appearing at about 4.7 eV. As hydrogen adsorbs onto the semiconductor surface, the intensities of the peaks at 1.9, 4.1 and 4.6 eV gradually decline to zero, while the intensity of the 3.1 eV band falls to about 20% of its original value. On the H-terminated surface, two broad negative bands are detected at 2.4 and 4.7 eV. In

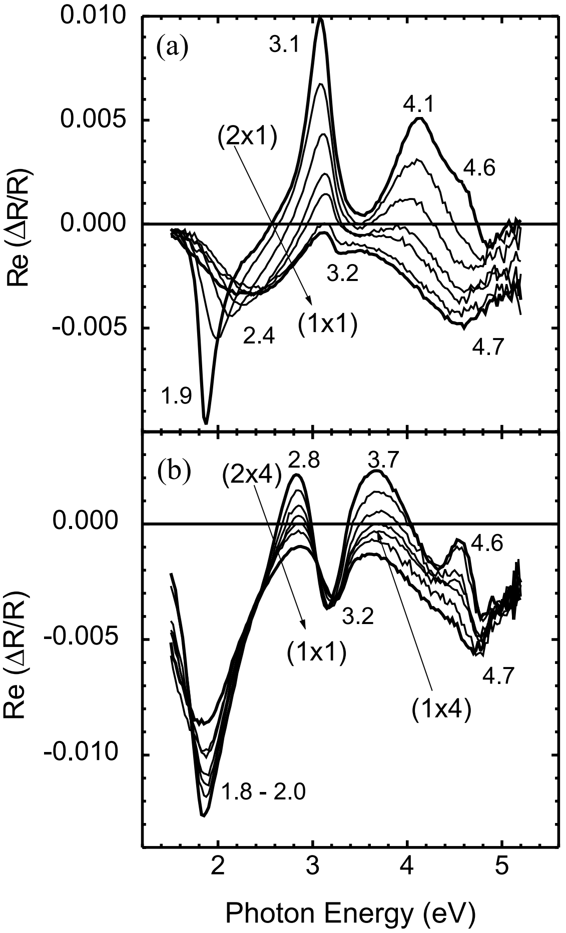

Fig. 1. Reflectance difference spectra of the InP(0 0 1) surface with increasing hydrogen dosage: (a) (2 × 1) and (b) $\delta(2\times4)$.

addition, a small negative peak at 3.2 eV can be discerned underneath the diminished 3.1 eV band. The RDS peaks observed on the clean and hydrogen-covered (2 × 1) surface are summarized in Table 1.

Fig. 1(b) shows a series of reflectance difference spectra recorded during hydrogen dosing of the $\delta(2\times4)$ reconstruction. The LEED pattern for this surface gradually changes from (2 × 4) to (1 × 4) at 300 L of H_2, then to (1 × 1) at 500 L of H_2. The RDS spectrum of the clean $\delta(2\times4)$ contains an intense negative band ranging from 1.8 to 2.0 eV, three small positive bands at 2.8, 3.7 and 4.6 eV, and two negative features at 3.2 and 4.7 eV. Upon dosing the crystal with hydrogen, the negative peak at 1.8–2.0 eV declines in intensity by about 40%, while the positive bands at 2.8, 3.7 and 4.6 eV gradually disappear. The negative peaks at 3.2 and 4.7 eV are not affected by hydrogen adsorption, and become the dominant features in the spectrum of the H:$\delta(2\times4)$.

In Fig. 2, the reflectance difference spectra of the hydrogen-saturated (2 × 1) and $\delta(2\times4)$ are com-

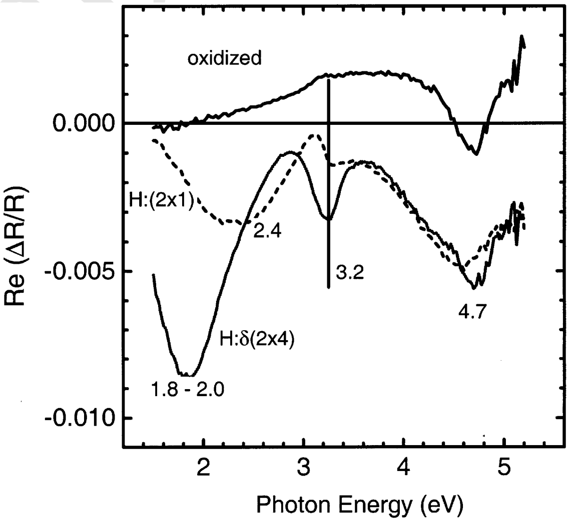

Fig. 2. Reflectance difference spectra of oxidized and hydrogen-terminated (2 × 1) and $\delta(2\times4)$ surfaces.

Table 1
Reflectance difference peaks on InP(0 0 1)

InP(0 0 1) surfaces	Photon energy (eV)										
	1.8	1.9	2.0	2.4	2.8	3.1	3.2	3.7	4.1	4.6	4.7
(2 × 1)		√				√	hidden		√	√	√
H:(2 × 1)				√		√–	√–				√
$\delta(2\times4)$	√		√		√		√	√		√	√
H:$\delta(2\times4)$	√		√				√				√

√: peak present in the spectra, √–: peak present in the spectra, but having a lower intensity.

pared to that of an oxidized InP(0 0 1) surface. Unlike the H:(2 × 1) and the H:$\delta(2 \times 4)$ surface, the oxidized surface does not exhibit negative optical anisotropy in the range from 1.5 to 3.0 eV. Above 3.5 eV, the RDS spectra of the H:(2 × 1) and H:(2 × 4) are very similar to each other, and show a negative peak at 4.7 eV that is also seen on the oxidized surface. Table 1 lists all the features recorded for the (2 × 1) and $\delta(2 \times 4)$ reconstructions, with and without adsorbed hydrogen.

Shown in Fig. 3 are the dependencies of the hydrogen coverage (θ_H) and the magnitude of the 4.1 eV peak ($\mathrm{Re}(\Delta R/R)$) on the amount of hydrogen dosed onto the (2 × 1) reconstruction. The H coverage at different dosages was determined separately by quantitative infrared spectroscopy [23,25]. A dose of 500 L of H_2 corresponds to approximately 1.0 L of H atoms. The amount of adsorbed hydrogen on the (2 × 1) rapidly increases with exposure up to 240 L of H_2, and then levels off to 1.0 ML at about 500 L. The decline in the absolute magnitude of the 4.1 eV RDS peak follows a trend that mirrors the hydrogen coverage. In fact, the peak height is directly proportional to the fraction of vacant sites, which equals $(1 - \theta_H)$. The linear relationship exhibited between the peak magnitude and the hydrogen coverage is observed for the other RDS features at 2.8, 3.1, 3.7, and 4.6 eV.

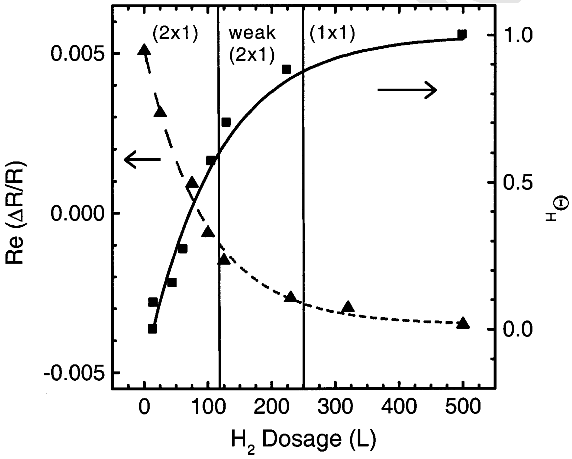

Fig. 3. The dependencies of the hydrogen coverage (■) and magnitude of the RDS peak at 4.1 eV (▲) on the hydrogen (H_2) exposure.

4. Discussion

4.1. Surface structure

To interpret the RDS spectra, we must now consider the atomic structure of the (2 × 1) and $\delta(2 \times 4)$ InP reconstructions. Shown in Fig. 4 are filled-states STM images of these surfaces that have been reported previously [23,26]. Examina-

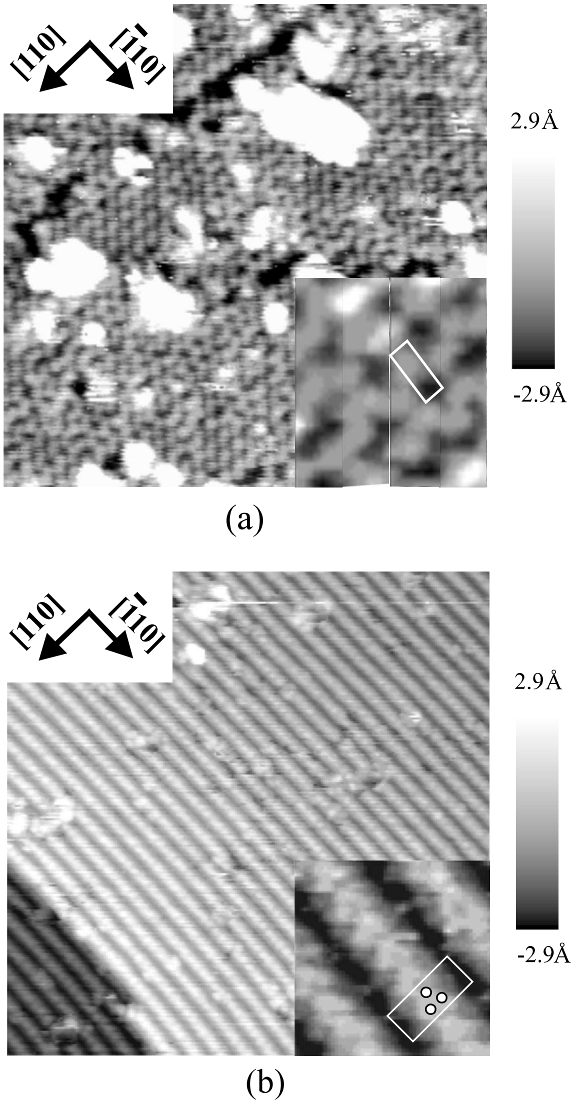

Fig. 4. Scanning tunneling micrographs of the (a) (2 × 1) (240 × 240 Å^2), and (b) $\delta(2 \times 4)$ (440 × 440 Å^2).

tion of the (2 × 1) picture reveals it consists of zigzagging rows of gray spots extending in the [1 1 0] direction [26,27]. The spots are associated with the filled dangling bonds on the phosphorus atoms. Each unit cell contains a single phosphorus dimer, and only one of the atoms on the dimer has a filled dangling bond. The white (or black) patches interspersed over the gray rows are small islands (or vacancies) of (2 × 1) termination that are two layers above (or below) the main terrace. The infrared spectrum of hydrogen adsorbed on this reconstruction exhibits vibrational bands due to PH and PH_2 species, but none for indium hydrides [26]. This confirms that the top layer is completely covered with phosphorus.

Present in Fig. 5(a) is a ball-and-stick model for the (2 × 1) surface. It is terminated with a complete layer of buckled phosphorus dimers with one dangling bond associated with each P atom. These atoms alternately contain a partially-filled and filled dangling bond (indicated by the small dots in the schematic). It is proposed that the phosphorus atom containing the filled electron pair is pushed up and appears bright in the STM image, while the phosphorus atom with the partially-filled dangling bond is pulled down and appears dark [26]. Strain induced by the dimer termination is minimized by having the up atom alternate between opposite ends of the dimer as one proceeds along the dimer row. This yields the zigzag pattern as observed in Fig. 4(a). Note that the (2 × 1) model does not satisfy the electron counting model [28].

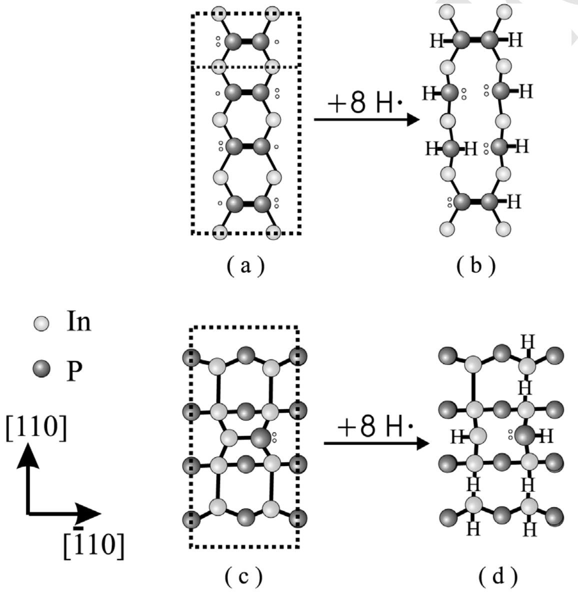

Fig. 5. Ball-and-stick models of InP(0 0 1) surface reconstructions: (a) (2 × 1), (b) H:(2 × 1), (c) $\delta(2 \times 4)$, and (d) H:$\delta(2 \times 4)$.

A ball-and-stick model for adsorbed hydrogen on the (2 × 1) phase is presented in Fig. 5(b). Hydrogen atoms attack the dangling orbitals and the dimer bonds generating different P–H_0 structures. In the model, five distinct configurations have been drawn. The first dimer at the top of the picture shows two P–H bonds that are vibrationally coupled through the dimer bond. The second dimer contains two P–H bonds that are weakly coupled through the interacting lone pairs. The third dimer is split into a PH_2 group and an isolated PH group. Finally, the fourth dimer contains an isolated PH group that is tethered to a dimer bond, instead of to a lone pair. Each of these hydrogen bond types yields distinct vibrational modes that have been identified in the infrared spectrum of the H:(2 × 1) [29]. Note that hydrogen adsorption does not necessarily reduce the number of filled dangling orbitals, nor does it eliminate all the dimer bonds.

The different types of bonding states present on the clean and hydrogen-covered (2 × 1) reconstruction are summarized in Table 2. The clean surface contains partially filled phosphorus dangling bonds, filled phosphorus dangling bonds, P–P dimer bonds, and P–In back bonds, whereas the H-terminated surface contains filled phosphorus dangling bonds, fewer P–P dimer bonds, P–In back bonds, and various P–H bonds.

Returning now to the indium-rich $\delta(2 \times 4)$ reconstruction, a filled-states STM image of this surface is shown in Fig. 4(b). One sees uniform gray rows extending along the [$\bar{1}$ 1 0] crystal axis. The inset image at a higher magnification reveals that each row contains three bright spots in the shape of an equilateral triangle that repeats every 8 Å. Recent ab initio, total-energy calculations indicate that this set of three spots is due to a mixed In–P dimer that sits astraddle four In–In dimers in the next lower layer [31]. One spot results from the filled dangling bond on the phosphorus atom,

Table 2
Surface bonds on InP(0 0 1)

InP(0 0 1) surfaces	Partially filled P–DB	Filled P–DB	P–P dimers	P–In back bonds	In–In back bonds	In–In dimers	In–P dimers	Empty In–DB	P–H bonds	In–H bonds
(2×1)	√	√	√	√						
H:(2×1)		√	√–	√					√	
$\delta(2 \times 4)$		√–		√–	√	√	√	√		
H:$\delta(2 \times 4)$		√–		√–	√	H-bridged		√–		√

DB: dangling bonds, √: bonds present on the surface, √–: bonds present on the surface, but with a reduced number as compare to the (2×1) surface.

while the other two spots are due to the In–In back bonds associated with the first and second layer indium atoms. Infrared spectroscopy of adsorbed hydrogen exhibit P–H and In–H stretching vibrations that are consistent with a surface covered with In–P and In–In dimers [23].

A ball-and-stick model of the $\delta(2 \times 4)$ reconstruction is presented in Fig. 5(c). Each (2×4) unit cell contains one In–P dimer that sits on top of four In–In dimers [31]. The $\delta(2 \times 4)$ model satisfies the electron counting model [28]. The phosphorus coverage on this surface is 0.125 monolayers, in contrast to 1.0 monolayers on the (2×1). Hydrogen atom adsorption generates the bond structures seen in Fig. 5(d). Each specific bond type shown in the model has been identified by analyzing the vibrational data with the aid of molecular cluster calculations [30]. On this surface, H atoms break the In–P dimer bonds, generating terminal P–H and In–H species. In addition, they insert into the In–In dimers, forming both terminal and bridged indium hydrides.

The valence bonds present on the clean and hydrogen-terminated $\delta(2 \times 4)$ surface are summarized in Table 2. On the clean (2×4), one finds filled phosphorus dangling bonds, P–In back bonds, In–In back bonds, indium dimer bonds, In–P dimer bonds, and empty indium dangling bonds. The number of filled phosphorus dangling bonds and P–In back bonds are reduced relative to the (2×1) reconstruction. By contrast, on the hydrogen-covered (2×4), there are filled-phosphorus dangling bonds, P–In back bonds, In–In back bonds, In–H–In bridging bonds, some empty indium dangling bonds, and terminal In–H bonds.

4.2. Comparison to RD spectra

A comparison of the surface states listed in Table 2 with the RDS bands identified in Table 1 makes it possible to associate the latter features with specific bonds present on the indium phosphide surface. The peaks at 1.9 and 4.1 eV in the RD spectrum of the (2×1) completely disappear upon hydrogen adsorption. Consequently, they most likely arise from transitions involving the partially filled phosphorus dangling bonds, since these are the only states that are eliminated by hydrogen termination. It should be noted that the ultraviolet photoemission spectrum of the (2×1) exhibits two peaks at 1.9 and 4.4 eV, in agreement with the RDS data [19,32].

The positive peak at 3.1 eV that appears in the optical spectra of the clean and hydrogen-terminated (2×1) may be assigned to a transition involving the phosphorus dimer bonds. Not all of these bonds are broken upon hydrogen adsorption, which is consistent with the ~80% decline in the peak intensity recorded following adsorption. Moreover, previous work has shown that the intensity of the 3.1-eV band is directly proportional to the coverage of phosphorus dimers [18]. On the H:(2×1), a broad negative band is detected at 2.4 eV that is most likely related to the P–H bonds.

As can be seen in Fig. 1(b), the most striking feature in the reflectance difference spectrum of the $\delta(2 \times 4)$ are the negative bands observed at 1.8 to 2.0 eV. Schmidt et al. [20] have calculated the optical anisotropy of this reconstruction, and concluded that these bands originate from transitions between the second-layer indium atoms and

In dimer bonds as well as empty In dangling bonds. Upon hydrogen adsorption, the intensity of this band decreases by 40%, indicating that these states have only been partially eliminated. This is consistent with our understanding of the H:$\delta(2 \times 4)$, which contains a significant number of empty indium dangling bonds after hydrogen adsorption.

The positive bands at 2.8 and 3.7 eV in the RD spectrum of the $\delta(2 \times 4)$ are probably related to the In–P dimers. It has been found that the H atoms attack and break all the In–P bonds [30]. Consistent with this, the 2.8 and 3.7 eV bands are completely eliminated upon hydrogen termination of the (2×4). The small peak recorded at 4.6 eV in the RD spectra of the (2×1) and $\delta(2 \times 4)$ is difficult to associate with a transition involving a specific valence state. It may be related to the filled phosphorus dangling bonds located on the P–P and In–P dimers. Alternatively, it may be due to bulk signal that is sensitive to surface states, as suggested by Nakayama et al. [33]. Finally, both reconstructions exhibit optical anisotropies at about 3.2 and 4.7 eV. These features are due to bulk transitions, since their energy matches the E_1 and E_0' interband critical points for indium phosphide [34].

The data shown in Fig. 3 indicate that the intensities of the RDS bands are strongly diminished when adsorbates are present on the InP(0 0 1) surfaces. This can explain some of the discrepancies reported in the literature. For example, when InP(0 0 1) crystals are transferred directly from the MOVPE reactor to the vacuum environment, the surface consists of a (2×1)-like structure that is covered with phosphorus ad-dimers, alkyl groups, and hydrogen atoms [21]. Intermediate spectra in Fig. 1(a) closely resemble the ‘weak c(4×4)’ RDS results obtained in MOVPE and other epitaxial growth processes [1–5]. In these studies, the optical data were collected either during dosing the crystal with phosphorus, or after cooling the sample to room temperature in a background pressure of the phosphorus precursor. For one to use reflectance difference spectroscopy as an in situ monitor of compound semiconductor surfaces during growth, the affect of adsorbates on the signal intensity must be carefully factored into the interpretation of the data.

5. Summary

In conclusion, the reflectance difference spectra of the InP(0 0 1) (2×1) and $\delta(2 \times 4)$ reconstructions have been examined using hydrogen as a probe of the surface bonds. Most of the observed spectral features can be associated with transitions involving specific surface valence states. Moreover, the intensities of the RDS peaks decrease in direct proportional to the hydrogen coverage.

Acknowledgements

Funding for this research was provided by the National Science Foundation, Divisions of Chemical and Transport Systems and Materials Research.

References

[1] T. Hannappel, S. Visbeck, K. Knorr, J. Mahrt, M. Zorn, F. Willig, Appl. Phys. A 69 (1999) 427.
[2] J.S. Luo, J.F. Geisz, J.M. Olson, M.-C. Wu, J. Cryst. Growth 174 (1997) 558.
[3] K.B. Ozanyan, P.J. Parbrook, M. Hopkinson, C.R. Whitehouse, Z. Sobiesierski, D.I. Westwood, J. Appl. Phys. 82 (1997) 474.
[4] P.J. Parbrook, K.B. Ozanyan, M. Hopkinson, C.R. Whitehouse, Z. Sobiesierski, D.I. Westwood, Appl. Surf. Sci. 123 (1998) 313.
[5] M. Zorn, T. Trepk, J.-T. Zettler, B. Junno, C. Meyne, K. Knorr, T. Wethkamp, M. Klein, M. Miller, W. Richter, L. Samuelson, Appl. Phys. A 65 (1997) 333.
[6] I. Kamiya, D.E. Aspnes, L.T. Florez, J.P. Harbison, Phys. Rev. B 46 (1992) 15894.
[7] A.I. Shkrebtii, N. Esser, W. Richter, W.G. Schmidt, F. Bechstedt, B.O. Fimland, A. Kley, R.D. Sole, Phys. Rev. Lett. 81 (1998) 721.
[8] M. Pristovsek, T. Trepk, M. Klein, J.T. Zettler, W. Richter, J. Appl. Phys. 87 (2000) 1245.
[9] J.R. Creighton, K.C. Baucom, Surf. Sci. 409 (1998) 372.
[10] M. Ebert, K.A. Bell, S.D. Yoo, K. Flock, D.E. Aspnes, Thin Solid Films 364 (2000) 22.
[11] S.E. Acosta-Ortiz, A. Lastras-Martínez, Phys. Rev. B 40 (1989) 1426.

[12] C. Goletti, C. Springer, U. Resch-Esser, N. Esser, W. Richter, B.O. Fimland, Phys. Rev. B 61 (2000) 1681.
[13] A.M. Frisch, W.G. Schmidt, J. Bernholc, M. Pristovsek, N. Esser, W. Richter, Phys. Rev. B 60 (1999) 2488.
[14] S.J. Morris, J.M. Bass, C.C. Matti, Phys. Rev. B 52 (1995) 16739.
[15] J.R. Power, P. Weightman, S. Bose, A.I. Shkrebtii, R.D. Sole, Phys. Rev. Lett. 80 (1998) 3313.
[16] L. Kipp, D.K. Biegelsen, J.E. Northrup, L.-E. Swartz, R.F. Bringans, Phys. Rev. Lett. 76 (1996) 2810.
[17] M.J. Begarney, L. Li, C.H. Li, C.D. Law, Q. Fu, R.F. Hicks, Phys. Rev. B 62 (2000) 8092.
[18] M.J. Begarney, C.H. Li, D.C. Law, S.B. Visbeck, Y. Sun, R.F. Hicks, Appl. Phys. Lett. 78 (2001) 55.
[19] T. Hannappel, L. Töben, S. Visbeck, H.-J. Crawack, C. Pettenkofer, F. Willig, Surf. Sci. 470 (2000) L1.
[20] W.G. Schmidt, N. Esser, A.M. Frisch, P. Vogt, J. Bernholc, F. Bechstedt, M. Zorn, T. Hannappel, S. Visbeck, F. Willig, W. Richter, Phys. Rev. B 61 (2000) R16335.
[21] L. Li, B.-K. Han, D. Law, C.H. Li, Q. Fu, R.F. Hicks, Appl. Phys. Lett. 75 (1999) 683.
[22] J. Kinsky, C. Schultz, D. Pahlke, A.M. Frisch, T. Herrmann, N. Esser, W. Richter, Appl. Surf. Sci. 123/124 (1998) 228.
[23] L. Li, Q. Fu, C.H. Li, B.-K. Han, R.F. Hicks, Phys. Rev. B 61 (2000) 10223.
[24] L. Li, B.-K. Han, S. Gan, H. Qi, R.F. Hicks, Surf. Sci. 398 (1998) 386.
[25] H. Qi, P.E. Gee, T. Nguyen, R.F. Hicks, Surf. Sci. 323 (1995) 6.
[26] L. Li, B.-K. Han, Q. Fu, R.F. Hicks, Phys. Rev. Lett. 82 (1999) 1879.
[27] P. Vogt, T. Hannappel, S. Visbeck, K. Knorr, N. Esser, W. Richter, Phys. Rev. B 60 (1999) R5117.
[28] M.D. Pashley, Phys. Rev. B 40 (1989) 10481.
[29] Q. Fu, D.C. Law, L. Li, C.H. Li, E. Negro, R.F. Hicks, Phys. Rev. B, submitted for publication.
[30] Q. Fu, L. Li, C.H. Li, D.C. Law, R.F. Hicks, JACS, submitted for publication.
[31] W.G. Schmidt, F. Bechstedt, N. Esser, M. Pristovsek, C. Schultz, W. Richter, Phys. Rev. B 57 (1998) 14596.
[32] A.M. Frisch, P. Vogt, S. Visbeck, T. Hannappel, F. Willig, W. Braun, W. Richter, J. Bernholc, W.G. Schmidt, N. Esser, Appl. Surf. Sci. 166 (2000) 224.
[33] T. Nakayama, M. Murayama, Jpn. J. Appl. Phys. 38 (1999) 3497.
[34] P. Lautenschlager, M. Garriga, M. Cardona, Phys. Rev. B 36 (1987) 4813.